AD-A121 410 AN EXPERIMENTAL INVESTIGATION OF MOLECULAR RAREFACTION EFFECTS IN GAS LUB..(U) COLUMBIA UNIV NEW YORK DEPT OF MECHANICAL ENGINEERING Y HSIA ET AL. FEB 81

UNCLASSIFIED N00014-75-C-0552 F/G 13/9 NL

END

FILMED

DTIC

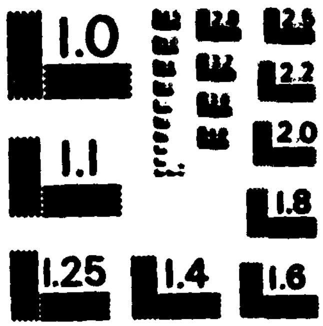

MICROCOPY RESOLUTION TEST CHART
NATIONAL BUREAU OF STANDARDS-1963-A

ASME

An Experimental Investigation of Molecular Rarefaction Effects in Gas Lubricated Bearings at Ultra-Low Clearances

Introduction

[illegible]

The study of ultra thin gas film bearings has become of great interest in recent years. The prime motivation has come from the computer magnetic disk recording industry where higher recording density and signal resolution can be achieved if the read write element which is attached to the [illegible] slider can be maintained at a closer spacing over the magnetic disk rotating at a high speed. Since the first conception and application of the disk recording head element in [illegible], the classical Reynolds equation has been found to predict well the performance of the air bearing operating with film thicknesses on the order of [illegible] µm [illegible]. The sliders studied [illegible] were either plane flat sliders or convex sliders with very large [illegible]

[illegible]

[1] Presently with Digital Equipment Corporation, [illegible]

[2] Presently with Xerox Corporation, [illegible]

Contributed by the Lubrication Division of The American Society of Mechanical Engineers for presentation at the ASLE-ASME Joint Lubrication Conference, New Orleans, La., [illegible] 1981. Manuscript received by the Lubrication Division [illegible] 1981. [illegible]

Copies will be available until June [illegible]

82 11 09 05[illegible]

[illegible]

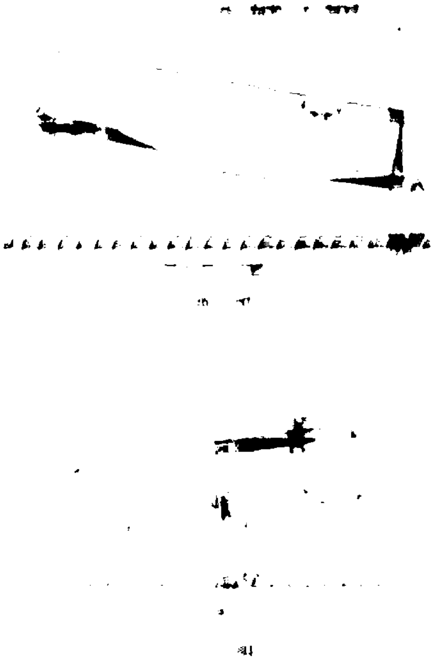

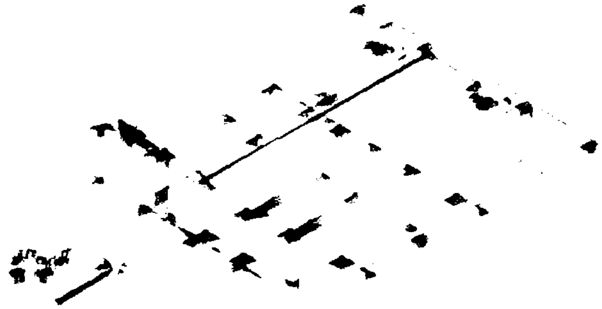

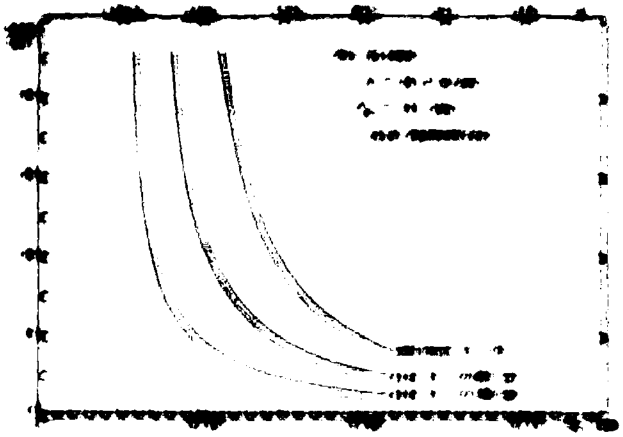

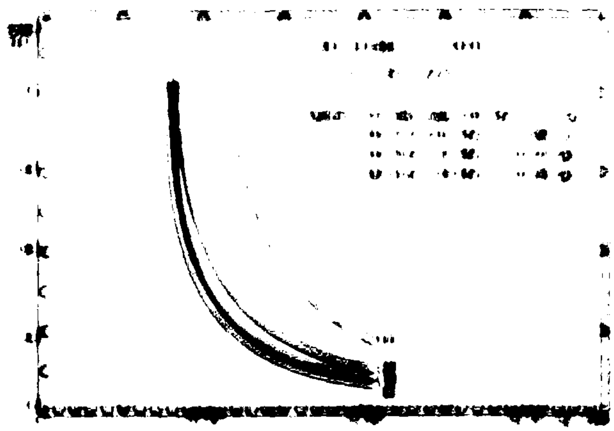

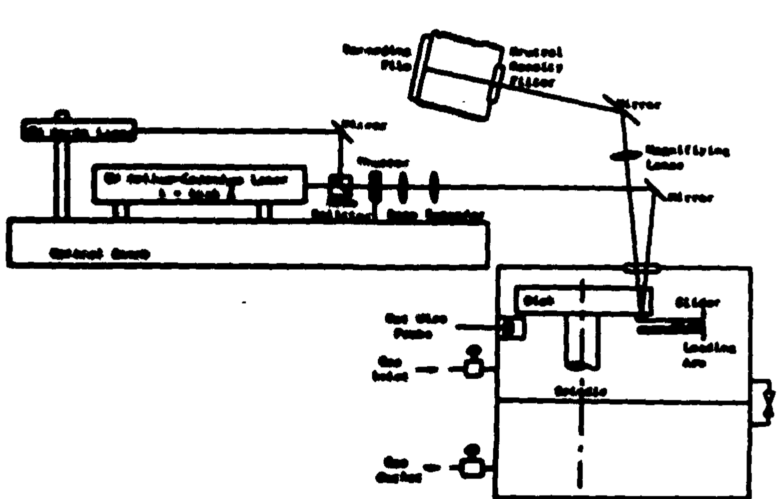

Fig. 6 Schematic diagram of interferometric setup

Equation (3) is written in slightly different form than the equation derived by [5] in that the ratio of the slider width to the slider length is present. Several observations can be made about equation (3). One is that if the bearing number, Λ, is "sufficiently" large and the width to length ratio is of order 1, the Couette term on the right-hand side of equation (3) will dominate while the molecular slip terms on the left-hand side of the equation can be neglected. However, if the slider is very narrow (width to length ratio of 0.1 or less), as is the case for the present bearing geometry, the transverse fluid flow (i.e., side leakage) cannot be neglected and the Couette term will no longer dominate. Therefore, the criterion for "large" bearing number is governed by a new dimensionless parameter, Λ^* ($= \Lambda(w/\ell)^2$). The dimensionless group will be referred to as the *modified bearing number*. Thus for narrow bearings, the flow inside the gas film will not be Couette dominant until the modified bearing number, Λ^*, is sufficiently large. Until this limit is reached, molecular slip effects in narrow bearing cannot be neglected even though the conventional bearing number is extremely high. However, the importance of the conventional bearing number cannot be neglected in light of the new modified bearing number because the magnitude of the conventional bearing number gives insight into the extent of the trailing edge boundary layer and governs the grid spacing requirements for a stable numerical solution. To reflect this importance, the conventional bearing number is therefore based on the trailing edge clearance and not on any other clearances.

Experimental Apparatus

Description of Apparatus. The experimental apparatus used in this investigation was originally designed and built by Strom [8]. Two major changes have been made to the experimental setup. First is that the variable wavelength pulsed dye laser has been replaced with a continuous wavelength (CW) Helium-Cadmium laser with a wavelength of 441.6 nm. It was found that the CW laser was more reliable and the lasing wavelength was known very accurately. Second is that the test chamber has been instrumented with a gas analyzer to measure the concentration of different gas media which may be introduced into the chamber. Only gases with sufficiently different thermal conductivity than air can be used. Figure 6 is a schematic diagram showing the experimental setup. Basically, the apparatus consists of two major components – a sealable and controllable test chamber and an optical bench. A detailed description of the apparatus can be found in references [8, 10].

In this investigation, the molecular rarefaction effects are studied by changing the operating gas medium from air to helium. This is accomplished by force feeding the upper test chamber with ultrapure grade helium gas. The chamber is instrumented with a constant temperature hot-wire anemometer which functions as a gas analyzer. Since helium has a thermal conductivity that is eight times higher than that of air, the hot-wire anemometer can easily detect the presence of helium. With proper calibration of the hot-wire probe, the actual concentration of the helium present inside the test chamber can be measured to an accuracy of 1 percent. To insure a "dust-free" environment, the test chamber is purged with clean air which has been passed through an "absolute air filter," a standard filtering machine used by the computer disk memory industry to purge their disk packs with clean air.

The major components of the optical bench are the two CW lasers of different wavelength. A Helium-Neon laser with a wavelength of 632.8 nm and a Helium-Cadmium laser with a wavelength of 441.6 nm are used to generate the two different fringe patterns required for determining the clearance (flying) profile of the slider bearing. The optical paths of the two laser beams are made collinear through a system of mirrors and a beam splitter as shown schematically in Fig. 6. The resulting interference fringe patterns are focused and recorded on Polaroid film. With minor adjustments, the optical arrangement can also be used with white light (similar to Lin's work [9]).

Description of Slider Bearing. The slider bearings used in this investigation are the "Winchester" type flying heads found in magnetic disk memory packs. The slider is made of sintered ferrite with its two skates lapped to a very smooth surface finish.

The physical dimensions of the slider are obtained by two measuring techniques. An optical microscope with 10X magnification is used to measure the overall dimensions of the slider and the pivot point location. The dimensions of the slider used in this investigation are summarized in Table 1.

Interferometric techniques are used to measure the taper (ramp) height and the surface crown heights since they are too small to be measured by the microscope. Both quantities are obtained by analyzing the interference fringe photographs taken during actual experiment. The accuracy on the ramp height is within one-half the laser wavelength; for He-Cd laser, the error is only 0.22 μm out of 9.0 μm.

Surface curvature (crown height) on the slider skate is also measured by analyzing the interference fringes. Several assumptions are made about the crown. One is that the crown, when present, is parabolic in shape with its vertex located at the center of the "land" section of the skate. The crown may

Table 1 Measured dimensions of sliders tested

HEAD ID	l (mm)	w (mm)	l_r (mm)	D (mm)	h_r (μm)	x_{piv} (mm)		h_c (μm)
PA3	5.552	0.419	1.135	2.718	10.12	2.41	A	0.051
							B	0.051
PA1	5.500	0.381	1.138	2.718	9.81	2.46	A	0.064
							B	0.102
R2	5.537	0.521	0.965	2.515	8.26	2.54	A	−0.051
							B	0.000
Y2	5.570	0.533	1.092	2.548	12.02	2.54	A	−0.064
							B	−0.051
W2	5.512	0.850	0.813	2.261	8.24	2.49	A	0.191
							B	0.152

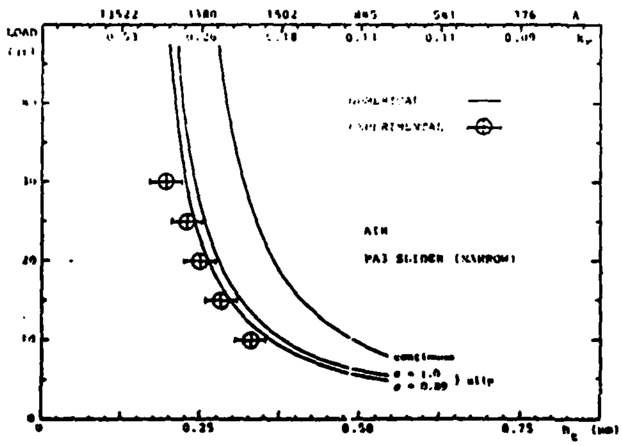

Fig. 7 Load versus trailing edge clearance, $U = 36.52$ m/s

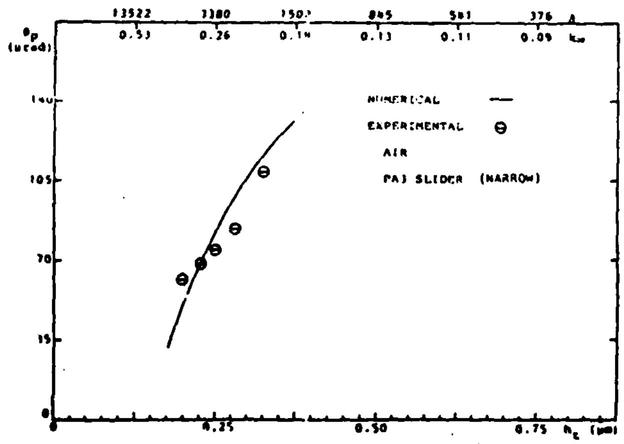

Fig. 9 Pitch angle versus trailing edge clearance, $U = 36.52$ m/s

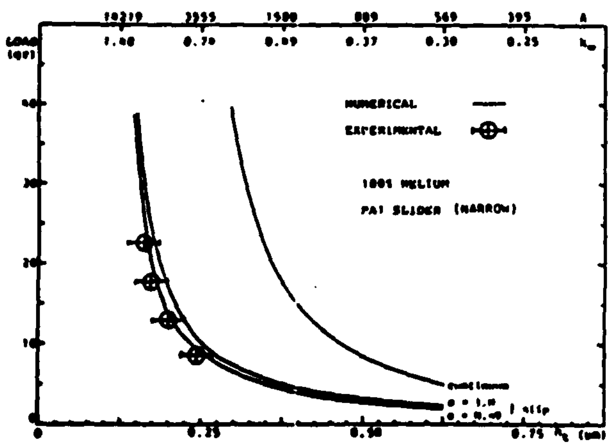

Fig. 8 Load versus trailing edge clearance, $U = 36.13$ m/s

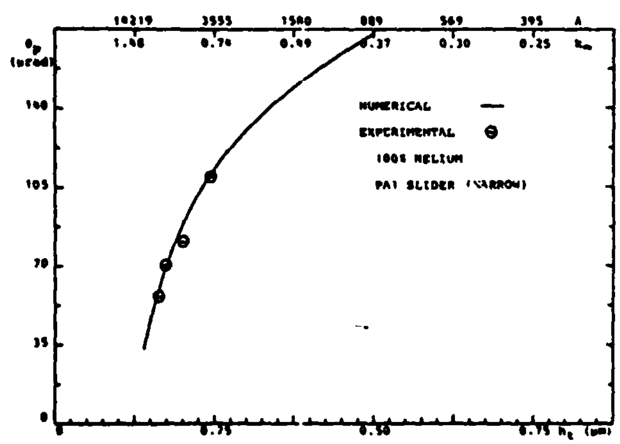

Fig. 10 Pitch angle versus trailing edge clearance, $U = 36.13$ m/s

be either concave or convex relative to the flat slider. The crowns on the two skates of the slider do not necessarily have to be the same in magnitude or concavity. The last column in Table 1 shows the extent of the variation in the crown height on each slider head. It is also assumed that the crown does not change in shape or in magnitude within the load range tested (from 10 to 30 grams.) Finally, there is no crown across the width of the skate.

It has been found that an inaccurate crown height determination will lead to an inaccurate flying profile determination, namely, the trailing edge clearance and the pitch angle. To minimize this error, the data reduction procedure for determining the surface curvature and the clearance profile has been lumped into one step with the use of a computer program. The detailed procedure can be found in reference [10]. Basically, the procedure involves the used of the Method of Least Squares to obtain the best fit of surface contour to all of the experimental data (fringe locations) for a given slider. The best fit contour determines the crown heights and the clearance profiles simultaneously. With this procedure, a 0.025 μm accuracy can be maintained in determining the trailing edge clearance.

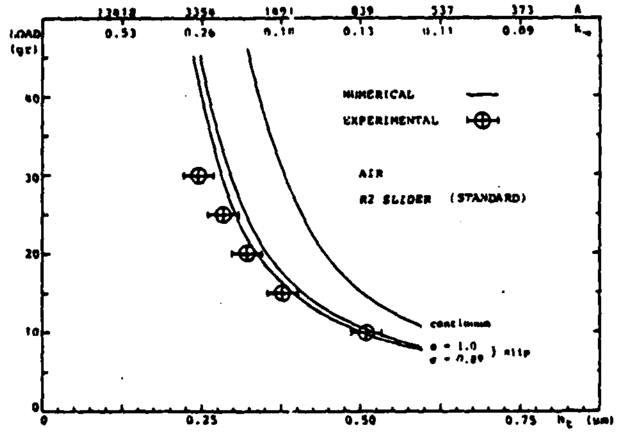

Fig. 11 Load versus trailing edge clearance, U = 36.13 m/s

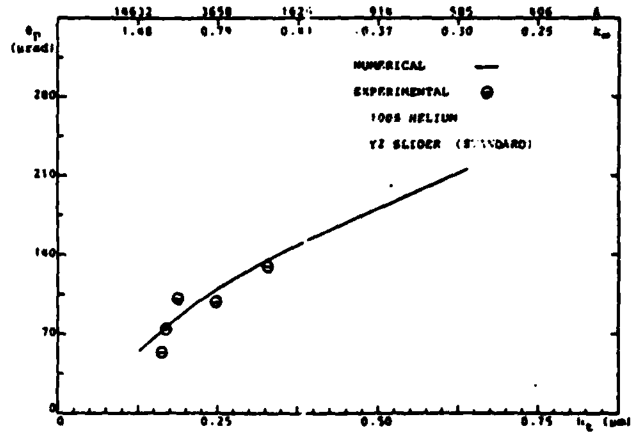

Fig. 14 Pitch angle versus trailing edge clearance, U = 36.71 m/s

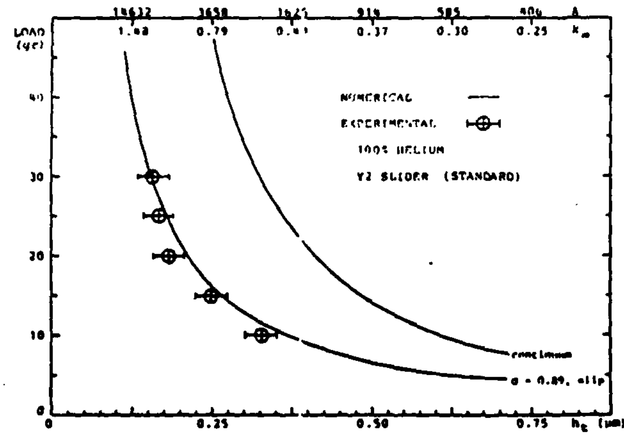

Fig. 12 Load versus trailing edge clearance, U = 36.71 m/s

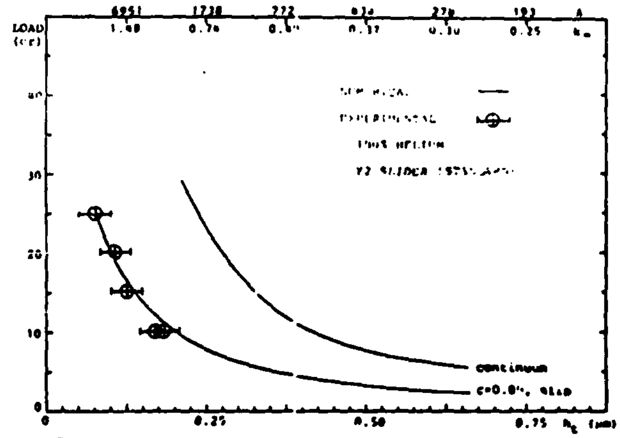

Fig. 15 Load versus trailing edge clearance, U = 17.43 m/s

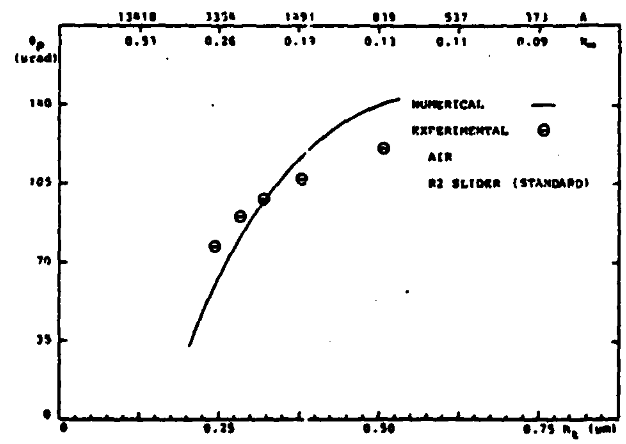

Fig. 13 Pitch angle versus trailing edge clearance, U = 36.13 m/s

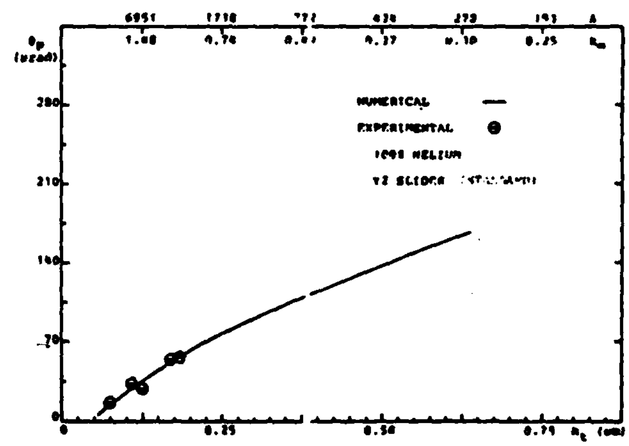

Fig. 16 Pitch angle versus trailing edge clearance, U = 17.43 m/s

Experimental Results and Comparison to Theory

In this investigation, the performance of Winchester heads of different rail widths – 0.38, 0.51, and 0.89 mm – are studied in both normal ambient air conditions and pure helium environment. The bearing velocities ranged from 17 to 52 m/s with external loads ranging between 8 to 30 grams. The clearance profile (trailing edge clearance, the pitch angle, and the roll angle) is determined interferometrically. In this investigation, extra precautions were taken to prevent the bearing from rolling. However, some rolling could not be avoided due to the differences in the surface contour of the two skates on each slider. Experimental load/spacing and pitch angle/spacing relations are then compared with numerical solutions of the modified Reynolds equation. The details of the numerical solution technique used in this investigation can be found in reference [10]. Theoretical predictions are based on actual physical dimensions of the sliders and not on the nominal design values. Gas properties of air and helium are assumed to be constant throughout the experiments; that is, air and helium viscosities are taken to be 18.27 and 19.5 Pa-s, respectively, while the mean free path are taken to be 0.069 and 0.188 μm, respectively. The ambient pressure is taken to be 101.4 kPa.

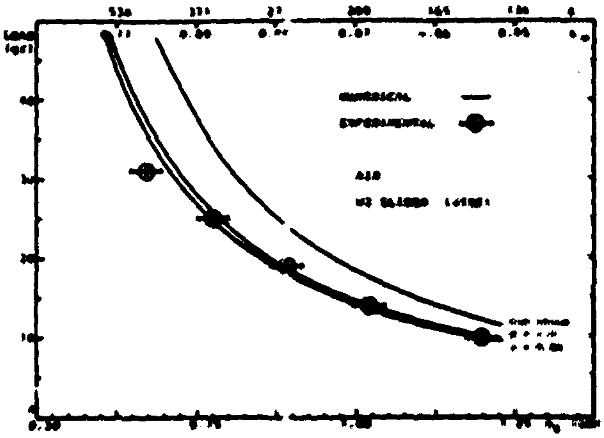

Fig. 17 Load versus trailing edge clearance, U = 38.13 m/s

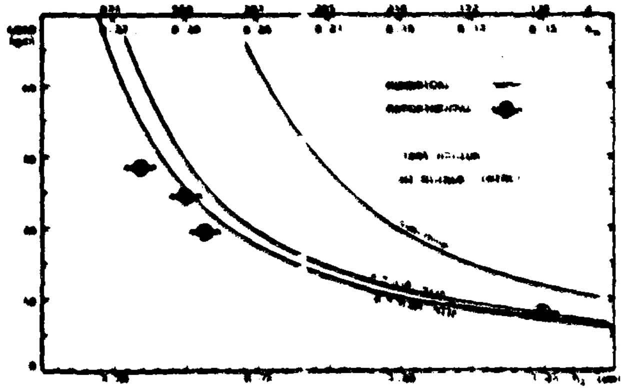

Fig. 18 Load versus trailing edge clearance, U = 36.38 m/s

To avoid confusion, the sliders used in this investigation are classified ac... ding to their widths – narrow, standard, and wide. Figures 7-10, Figs. 11-16, and Figs. 17-20 show the typical experimental results for the narrow, standard, and wide sliders, respectively, in both air and helium at a velocity 36 m/s. Also plotted on these figures are the theoretical results from the modified Reynolds equation. All theoretical curves presented are calculated based on a surface accommodation coefficient, σ, of 0.89 unless otherwise indicated.

Narrow Sliders. Figures 7 and 8 represent the typical experimental load/spacing relationship for the narrow sliders in air and helium, respectively, at the same disk velocity. Figures 9 and 10 show the pitch angle/spacing relationship associated to the two cases presented in Figs. 7 and 8, respectively.

Several important observations can be made from examining Figs. 7 and 8. To illustrate the effects of molecular slip, theoretical curves based on continuum theory and slip theory are also plotted on the two figures. As the figures clearly indicate, the main effect of slip is to decrease the load carrying capacity of the slider bearing as demonstrated by the fact that the slip theory curve always lies below the continuum theory curve. As expected, the effect of slip is greater in helium than in air since the mean free path of helium is larger. In addition, the two figures also show that even though the conventional bearing number (indicated by the upper scale on the figures) is of the order 10^3 to 10^4, the effects of slip and side leakage cannot be neglected. If high bearing number effects had dominated, the slip-flow theory curves and the continuum theory curves would have coincided, as was the case reported by Tseng [2]. At first, this may seem to be a surprising result; but if the *modified* bearing number (defined earlier) is used, it would be obvious that the bearing number is far from approaching the "high" bearing number range. In fact, for the narrow slider, the modified bearing number is only on the order of 10^1 to 10^2.

Figures 7 and 8 also show the effects of different values of surface accommodation coefficient, σ, on the theoretical predictions. Two values of σ were used, 1.0 and 0.89. As the figures show, slip theory with σ = 0.89 gives a slightly better agreement with experiment for both air and helium. The surface accommodation coefficient for air/glass interface was measured to be 0.89 [11], and Tseng [2] has shown that with this value, a better experimental/theoretical agreement can be achieved. However, there are no published data on σ for helium/glass interfaces. In the present investigation, different values were tested and the best agreement is obtained with σ = 0.89. It is believed that this value should be used for all future studies involving helium when using the first order approximation model.

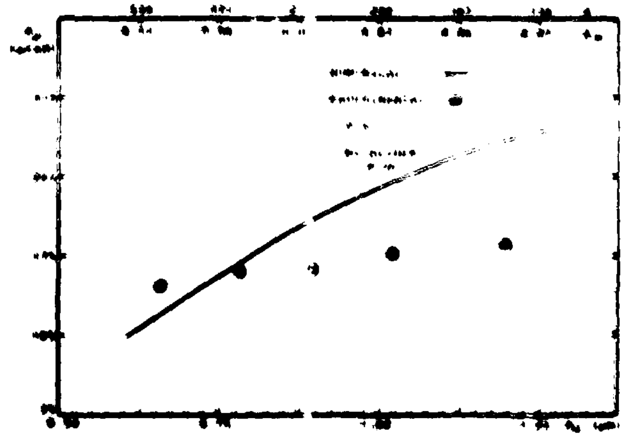

Fig. 19 Pitch angle versus trailing edge clearance, U = 38.13 m/s

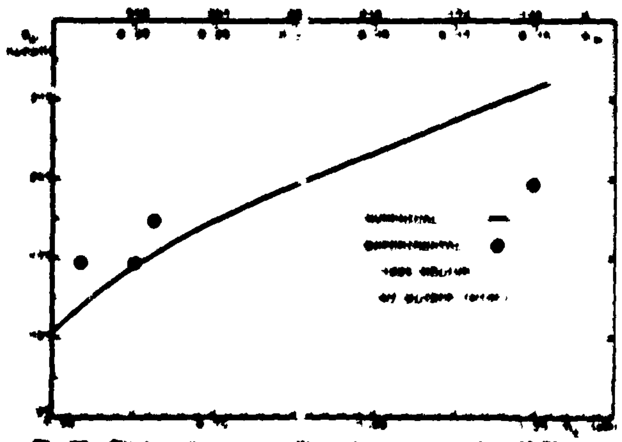

Fig. 20 Pitch angle versus trailing edge clearance, U = 38.38 m/s

Further examination of Figs. 7 and 8 shows that as the bearing clearance is decreased by increasing the external load, the agreement between theory and experiment does not deteriorate even as ambient Knudsen number is increased from 0.1 to 0.38 for air and 0.6 to 1.14 for helium. Moreover, helium results are in better agreement with the theory than air results. This phenomenon can be attributed to the fact that helium is a monatomic gas while air is a mixture of gases and that the slip-flow theory is derived with the assumption that the fluid is an ideal gas.

Examination of Figs. 9 and 10 shows that the slip theory also predicts the pitch angle of the slider bearing in both air helium with good accuracy. This can be attributed to the

accurate d[illegible]ion procedure used in the experimental study and the numerical scheme.

Standard Slider. Figures 11 and 12 show the typical experimental load/spacing relationship for the standard size slider operating at the same velocity as in Figs. 7 and 8. Figures 13 and 14 show the pitch angle/spacing relationships corresponding to the cases presented in Figs. 11 and 12, respectively. Once again, the agreement between theory and experiment is excellent, especially for helium.

An extremely high ambient Knudsen number of 2.4 was achieved by operating the standard slider at a velocity of 17.4 m/s in helium. The load/spacing and the pitch angle/spacing results are presented in Figs. 15 and 16. As Fig. 15 shows, a trailing edge clearance of 0.075 microns was achieved. The ambient Knudsen number associated with this low clearance is 2.4, while the conventional operating bearing number based on the trailing edge clearance is 19,300. It should be noted that even at this extremely high bearing number and high Knudsen number, the effects of the slip are still substantial since, as shown by the figure, the slip theory and continuum theory curves do not coincide. This is not a surprising result because the *modified* bearing number is only [illegible]. Until the [illegible] is large enough, the effects of molecular slip will continue to be [illegible].

Wide Sliders. Typical wide slider results at the same operating speed are presented in Figs. 17 to 20. Once again, the agreement between experiment and theory is excellent, especially for the helium cases. The scatter in the pitch angle measurements (Figs. 19 and 20) can be attributed to the fact that the bearing surfaces were extremely irregular and the surface contours assumed for data fitting were only rough approximations of the actual contour.

Comparing Figs. 7, 11, and 17 to 8, 12, and 18, one can see that the wide slider operates at much higher clearances than the narrow slider even though the wider slider is only twice as wide as the narrow bearing.

Discussions

Results of the present study clearly show that the modified Reynolds equation with slip flow approximation can predict accurately the change in the bearing clearance profile (i.e., the trailing edge clearance and the pitch angle) for a given fixed external load. The agreement between slip theory and the experiment is excellent for low ambient Knudsen numbers ($K_a < 0.1$), moderate Knudsen numbers ($0.1 < K_a < 0.5$) and high Knudsen numbers ($0.5 < K_a < 2.4$). It is somewhat misleading to use the ambient Knudsen number as a measure of molecular slip since the mean free path of the gas inside the gas film is smaller than the ambient value due to the fact that the local pressure is higher. Thus, the local Knudsen number, K_L, based on the local mean free path and local clearance, will be more representative of the actual molecular slip effect in the bearing system.

Figure 21 is a typical three-dimensional plot of the local Knudsen numbers under a narrow slider operating in air while Fig. 22 is a plot for a standard slider operating in helium. As the figures show, the local Knudsen numbers in the "land" section of the slider are considerably less than the "ambient" Knudsen number, especially in the helium case (Fig. 22). However, even with this dramatic decrease, the Knudsen number is nearly constant throughout the land region. Furthermore, in the helium case (Fig. 22), even though the ambient Knudsen number is 2.4, the bearing sees a much smaller local Knudsen number (around 0.9). This is exactly the consequence sought by this study, that is, high (local) Knudsen number effects in gas bearings. It is noted that the effects of slip are still substantial even with (conventional) bearing numbers of 6[illegible] and 19,300 for the two cases shown.

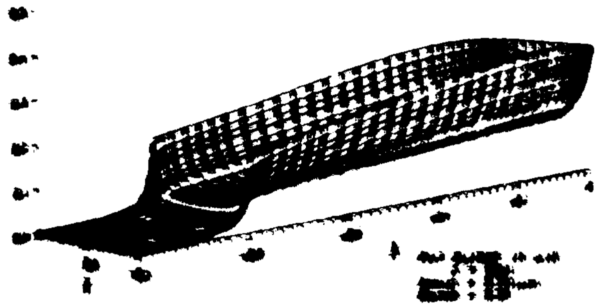

Fig. 21 Local Knudsen number distribution under a narrow slider (air)

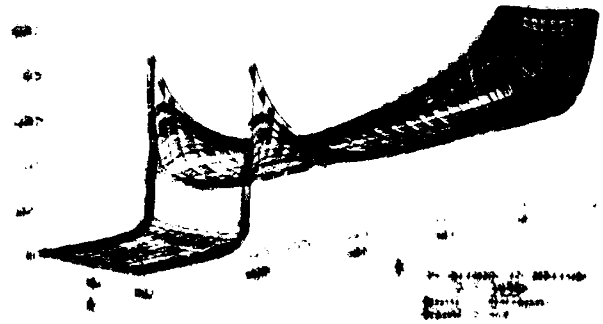

Fig. 22 Local Knudsen number distribution under a standard slider (helium)

In this investigation, the effects of slip have been conclusively studied by operating the sliders in regimes where the high bearing number effects are not dominant. Had the high bearing number effects been large, the effects of slip would be diminished. Moreover, there would be a small boundary layer formed at the side edges of the slider, and the pressure profile would be very flat across the width of the bearing and uniform through the length of the slider [[illegible]]. Figures 23 and 24 show typical pressure fields generated under a narrow slider in air and a standard slider in helium, respectively, at high conventional bearing numbers. It is clear from the two pressure contours that there are no signs of a side boundary layer present since there are no sharp pressure gradients near the edges. It should be noted that in Fig. 24 the severe decrease in pressure immediately after the slider taper is due to the concave crown that is present on the slider shoe (Fig. [illegible]). The effects of the crown on the bearing performance is more pronounced in this case because the crown height and the bearing clearance are nearly the same in magnitude. Consequently, when the slider is flying at such a low trailing edge clearance (0.075 µm), the concave crown effectively increases the overall bearing clearance and causes the pressure to decrease. If the concavity is sufficiently large, a subambient pressure area can develop, and this is probably the phenomenon occurring in the new [illegible] zero-load or [illegible] sliders.

In this investigation, the agreement between experiment and slip-flow theory is consistently better for helium results than for air results. It is theorized that this phenomenon is a direct result of the fact that helium is a monatomic gas while air is a mixture of polyatomic gases. Since the slip-flow theory is derived based on the assumption of ideal gas, the theory should predict better for "simple" gases, especially at the higher Knudsen numbers. Bird [[illegible]] has noted that in transition flow, a gas mixture may be initially in uniform composition, but species separation may occur due to thermal or pressure gradients. Since air is 78 percent nitrogen, a numerical experiment was performed using nitrogen gas properties, and a slightly better agreement between theory and experiment was achieved for all the "air" cases.

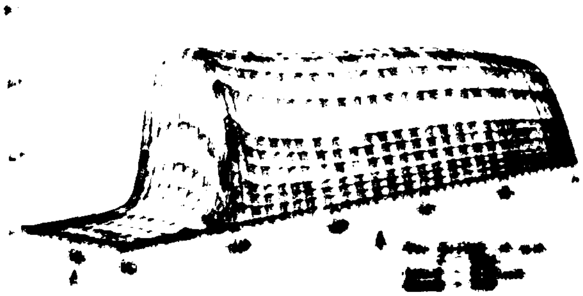

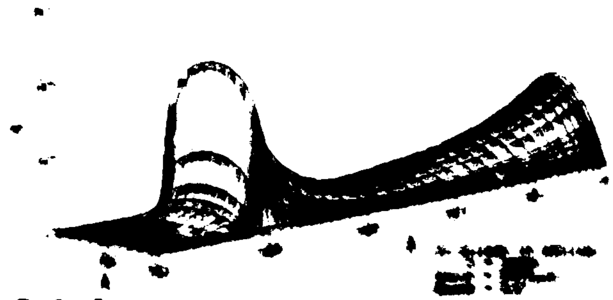

[illegible] the second order term [illegible] the slip-flow velocity when the local Knudsen number approaches unity. [illegible]

The approximate form of the Navier-Stokes equations [illegible] as follows:

$$[illegible] \qquad (A\text{-}5)$$

The corresponding boundary conditions for the [illegible] are as follows:

$$[illegible]$$

$$[illegible] \qquad (A\text{-}6)$$

Solving equations (A-5) for [illegible] with the boundary conditions (A-6), the following equations are obtained:

$$[illegible] \qquad (A\text{-}7)$$

$$[illegible] \qquad (A\text{-}8)$$

Upon evaluating equation (A-[illegible]) [illegible] one sees that the effect of the second order slip term is to [illegible] the slip velocity at the boundaries as the local Knudsen number approaches unity. [illegible]